Am J Cancer Res 2019;9(10):2156-2169
www.ajcr.us /ISSN:2156-6976/ajcr0102324

Original Article

Development and validation of a m^{6}A RNA methylation regulators-based signature for predicting the prognosis of head and neck squamous cell carcinoma

Xinyuan Zhao[1], Li Cui[2]

[1]*Stomatological Hospital, Southern Medical University, Guangzhou 510280, China;* [2]*UCLA School of Dentistry, Los Angeles, CA 90095, USA*

Received September 15, 2019; Accepted September 25, 2019; Epub October 1, 2019; Published October 15, 2019

Abstract: Head and neck squamous cell carcinoma (HNSCC) is among the most common types of cancers that threat the public health worldwide. A growing body of evidence has demonstrated that m^{6}A RNA methylation plays a critical role in tumorigenesis. However, the association between m^{6}A RNA methylation regulators and prognosis of HNSCC remains poorly known. This study aimed to construct a m^{6}A RNA methylation regulators-based biomarker signature that efficiently predicted the prognosis of HNSCC. The gene expression profile of m^{6}A RNA methylation regulators and the corresponding clinical information were downloaded from The Cancer Genome Atlas (TCGA) HNSCC dataset. The differentially expressed m^{6}A RNA methylation regulators between tumor samples and normal control samples, as well as the interaction and correlation of m^{6}A RNA methylation regulators were evaluated. Consensus clustering analysis was performed to identify the clusters of HNSCC with different clinical outcome. Then a prognostic signature was built on TCGA HNSCC cohort and further validated in an external independent cohort. The expression levels of METTL3, YTHDF1, KIAA1429, ALKBH5, YTHDF2, METTL14, FTO, WTAP, RBM15 and HNRNPC were significantly upregulated in tumor samples, while YTHDC2 was remarkably downregulated in the cancer specimens. WTAP and METTL14 might be the hub genes of the interaction network among m^{6}A RNA methylation regulators. Two clusters of HNSCC cases were identified and significant differences were found with respect to overall survival (OS) and tumor grade between the two subgroups of patients. A two-gene prognostic signature including YTHDC2 and HNRNPC was constructed and could predict OS in HNSCC patients from TCGA dataset. In addition, the prognostic signature-based risk score was identified as an independent prognostic indicator for HNSCC. More importantly, these findings were successfully validated in an external independent HNSCC cohort. In conclusion, our study has built up a robust m^{6}A RNA methylation regulators-based molecular signature that predicts the prognosis of patients with HNSCC with high accuracy, which might provide important guidance for therapeutic strategies.

Keywords: Head and neck squamous cell carcinoma, prognostic signature, survival analysis, m^{6}A RNA methylation

Introduction

Head and neck squamous cell carcinoma (HNSCC) is the sixth most frequent type of malignant tumors worldwide [1]. It arises from the epithelium lining the upper aerodigestive tract including the oral cavity, pharynx, and larynx. Genetic mutation, environment exposure, viral infection and unhealthy lifestyle are the common risk factors for HNSCC. Although the treatment modalities have been greatly improved in the past few decades, the 5-year overall survival rate for HNSCC remains dismal [2]. If diagnosed at the early stage, HNSCC is usually curable. However, most patients present in advanced stages with metastases when the therapies might be futile or aggressive treatment is required [3, 4]. Predicting prognosis of HNSCC with high accuracy is critical for successful clinical managements and personalized medicine. Currently the Tumor, Node, Metastasis (TNM) staging system is still the most extensively used prognostic indicator for monitoring HNSCC progression. However, it is very common to observe the phenomenon that the clinical outcome of patients at the same TNM stage is significantly different. Therefore, identification of novel and reliable prognostic molecular signatures is important for the selection of most appropriated therapeutic strategies and

improving the unfavorable prognosis of patients with HNSCC.

N6-methyladenosine (m^6A), methylated at the N6 position of adenosine, is the most prevalent internal modification that occurs in the mRNAs and long noncoding RNA (lncRNA) in many eukaryotic species, such as yeast, plants, flies and mammalians [5, 6]. m^6A methylation affects almost every aspect of RNA metabolism including, but not limited to, abundance, alternative splicing, stability, nuclear export, decay and translation [7]. Its regulatory effects are modulated by the dynamic interactions among its methyltransferases ("writers"), demethylases ("erasers") and binding proteins ("readers") [8]. m^6A methylation is actively involving in many important physiological processes such as stem cell differentiation and pluripotency, circadian periods, embryogenesis and DNA damage response [9-12]. Accumulative evidence has demonstrated that abnormal m^6A methylation modification is closely linked many human diseases including cancer [13]. For instance, downregulation of the methyltransferases METTL3 or METTL14 significantly promoted the malignant behaviors of glioblastoma stem cell (GSCs). Opposite findings were observed when demethylase FTO was suppressed. Mechanistically, knockdown of METTL3 or METTL14 promoted ADAM19 expression by affecting its m^6A enrichment [14]. The expression level of YTHDF2 was dramatically upregulated in pancreatic cancer tissues, and its levels were significantly higher in patients at the advanced stages [15].

The Cancer Genome Atlas (TCGA) is a large-scale and landmark cancer genomics program which has comprehensive and multi-dimensional data spanning 33 types of cancer [16]. Currently, the correlation between m^6A RNA methylation regulators and prognosis of HNSCC remains unclear. In this study, we first identified the significantly differentially expressed m^6A RNA methylation regulators between tumor and normal samples from TCGA HNSCC dataset. The interaction and correlation among the m^6A RNA methylation regulators were evaluated. Based on the expression pattern of m^6A RNA methylation regulators, consensus clustering analysis identified two clusters of HNSCC with different clinical outcome. Then a two-gene risk signature was built on TCGA HNSCC cohort and showed good performance for predicting prognosis. More importantly, this robust prognostic signature was successfully validated in another independent external HNSCC cohort.

Materials and methods

Public data source

The RNA-seq transcriptome data and corresponding clinical information of HNSCC samples as well as the RNA-seq transcriptome data of normal control samples were downloaded from The National Cancer Institute Genomic Data Commons (NCI-GDC) (https://gdc.cancer.gov/). The RNA-seq data have been normalized by Expectation-Maximization (RSEM) approach. A total of 502 HNSCC cases and 44 normal control samples were included for subsequent analysis.

Data pre-processing and differential expression analysis of m^6A RNA methylation regulators

EdgeR package was used for screening the differentially expressed genes (DEGs) between cancer samples and normal control samples. The adjusted $P < 0.05$ (calculated by Benjamini & Hochberg procedure) and absolute $\log_2FC > 1$ were chosen as the cut-off threshold. The analyzed results of thirteen currently known m^6A RNA methylation regulators including METTL3, YTHDF1, KIAA1429, YTHDC2, ALKBH5, YTHDF2, YTHDC1, ZC3H13, METTL14, FTO, WTAP, RBM15 and HNRNPC were obtained.

PPI network construction and correlation analysis

The STRING database (http://string-db.org) was used for analyzing the protein-protein interaction (PPI) among m^6A RNA methylation regulators. Pearson correlation analysis was employed to reveal the association among different m^6A RNA methylation regulators.

Consensus clustering analysis

To determine whether the expression levels of m^6A RNA methylation regulators were associated with prognosis, the TCGA HNSCC cohort was clustered into different groups by consensus expression of m^6A RNA methylation regulators with "ConsensusClusterPlus" in R. The overall survival (OS) difference between different clusters was calculated by the Kaplan-Meier meth-

Table 1. The clinical information of the validated HNSCC cohort

Clinicopathological features	Number
Age	
Mean (SD)	60.25 (12.92)
Gender, n (%)	
Male	156 (66.10%)
Female	80 (33.90%)
Pathological diagnosis	
Squamous cell carcinoma	236 (100%)
Tumor grade	
G1	53 (22.46%)
G2	103 (43.64%)
G3	67 (28.39%)
G4	13 (5.51%)
TNM stage	
Stage I	65 (27.54%)
Stage II	91 (38.56%)
Stage III	45 (19.07%)
Stage IV	35 (14.83%)

od and log-rank test. Chi-square test was used to compare the distribution of age, gender, grade and stage between different clusters.

Prognostic signatures generation and prediction

Univariate Cox analysis was performed to evaluate the correlation between m^6A RNA methylation regulators and overall survival for TCGA HNSCC cohort using survival analysis in R. The hazard ratios (HRs) of genes that larger than 1 were considered as risky genes, while those less than 1 were regarded as protective genes. A two-gene prognostic signature (YTHDC2 and HNRNPC) was identified. Multivariate Cox regression analysis and akaike information criterion (AIC) method were used to determine the optimal model. A risk score for each patient was calculated as the sum of each gene's score, which was obtained by multiplying the expression of each gene and its coefficient. The TCGA HNSCC cohort was stratified into high-risk group and low-risk group based on the median value of the risk scores. The difference of OS between high-risk group and low-risk group was calculated by the Kaplan-Meier method with a two-sided log-rank test. Receiver operating characteristic (ROC) curve was constructed to evaluate the prediction accuracy of the prognostic model. Chi-square test was performed to compare the distribution of clinicopathological parameters between high and low-risk group. Heatmaps were used to visualize the difference with pheatmap R package. Univariate and multivariate Cox regression analyses were used to identify the independent prognostic factors for the TCGA HNSCC cohort. The survival difference between high-risk group and low-risk group stratified by age, gender, grade and stage was further evaluated.

The validation patient cohort

The validation study was approved by the Ethic Committee of the Stomatological Hospital, Southern Medical University. The study specimens comprised of 236 patients with HNSCC. All the cases were pathologically confirmed. The detailed clinicopathological information of the validated HNSCC cohort was summarized in **Table 1**. Written informed consent was obtained from all the participants for the use of their tissue specimens.

Real-time PCR

The RNA purification kit (Quick-RNA MicroPrep, Zymo Research Corp., Irvine, CA, USA) was used to extract the total RNA was extracted from tissue specimens based on the manufacturer's instructions. Then SuperScript III Reverse Transcriptase (Invitrogen, Carlsbad, CA, USA) was employed to synthesize the complementary DNAs (cDNAs). The amplification of cDNAs were conducted with Light Cycler 480® SYBR Green I Master Mix (Roche, Applied Science, Indianapolis, IN, USA) using the CFX96 Real-Time PCR detection system (Bio-Rad Laboratories Inc., Hercules, CA, USA). Gene expression was normalized against GAPDH and relative expression levels of YTHDC2 and HNRNPC were determined by the $2^{-\Delta\Delta Ct}$ method. The cycling conditions were as follows: 95°C for 5 min, 40 cycles of 95°C for 15 sec, 56°C for 30 sec and 72°C for 30 sec, and 95°C for 60 sec.

Validation of the prognostic signature

Similarly, the validated HNSCC cohort was grouped to high-risk group and low-risk group based on their risk scores. Then the difference in OS was calculated, and the associations between risk score and the clinicopathological parameters of the validated HNSCC cohort were evaluated. Univariate and multivariate

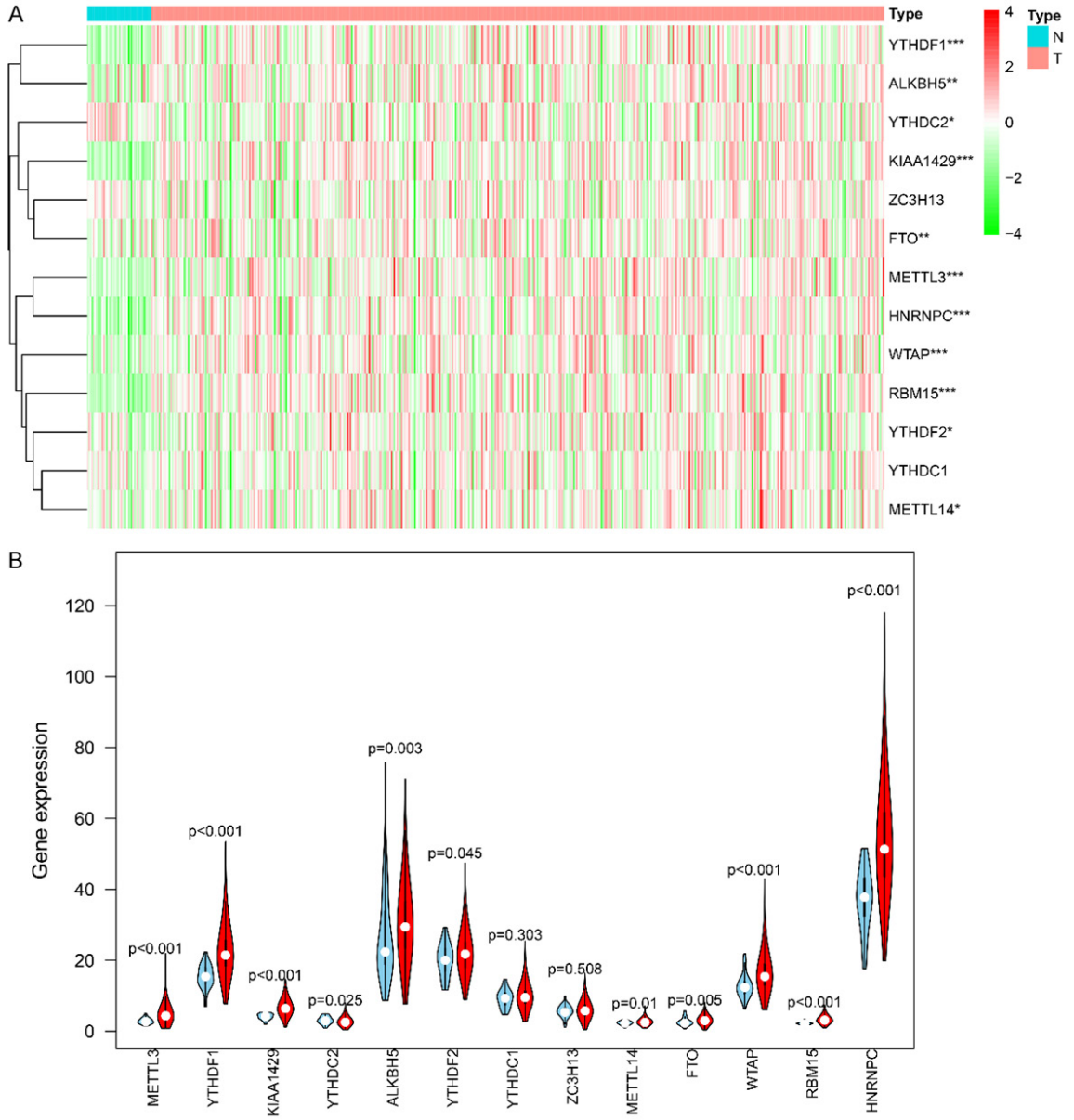

Figure 1. The expression levels of m^{6}A RNA methylation regulators between tumor samples and normal control samples in TCGA HNSCC cohort. A. The heatmap was used to visualize the expression levels of m^{6}A RNA methylation regulators in each clinical sample. B. The significantly differentially expressed m^{6}A RNA methylation regulators between tumor samples and the normal control samples.

Cox regression analyses were used to determine whether risk score was an independent prognostic factor. The survival difference between high-risk group and low-risk group stratified by clinicopathological parameters was also examined.

Statistical analysis

Data analysis was performed with the GraphPad Prism 7.0 (GraphPad, San Diego, CA, USA). All statistical tests were two-sided. A *P* value of less than .05 was considered statistically significant.

Results

The differentially expressed m^{6}A RNA methylation regulators between tumor samples and normal control samples

Heatmap was generated to visualize the expression pattern of m^{6}A RNA methylation regulators between HNSCC cases and normal con-

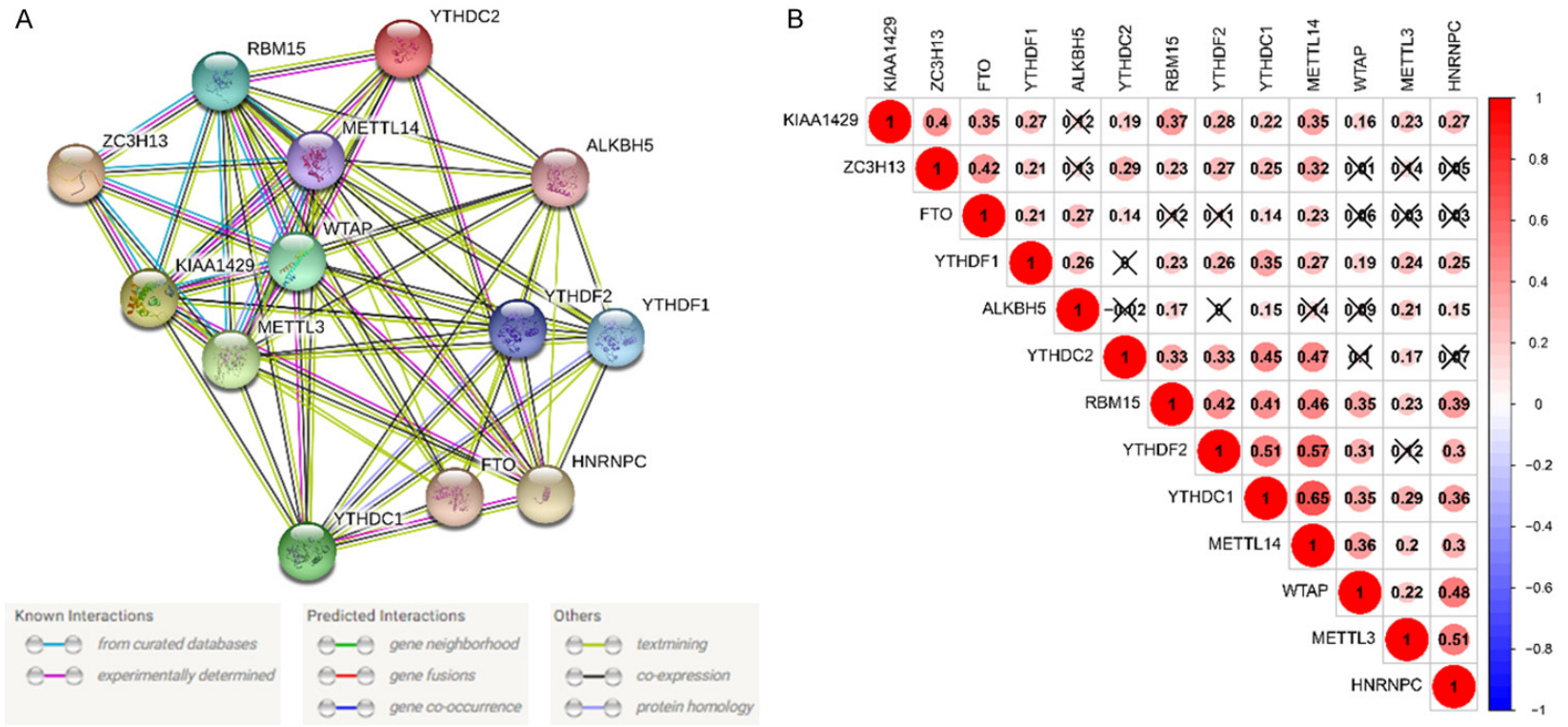

Figure 2. The interaction and correlation among m^{6}A RNA methylation regulators. A. PPI network was constructed to evaluate the interaction among m^{6}A RNA methylation regulators. B. The Pearson correlation analysis was used to determine the correlation among m^{6}A RNA methylation regulators.

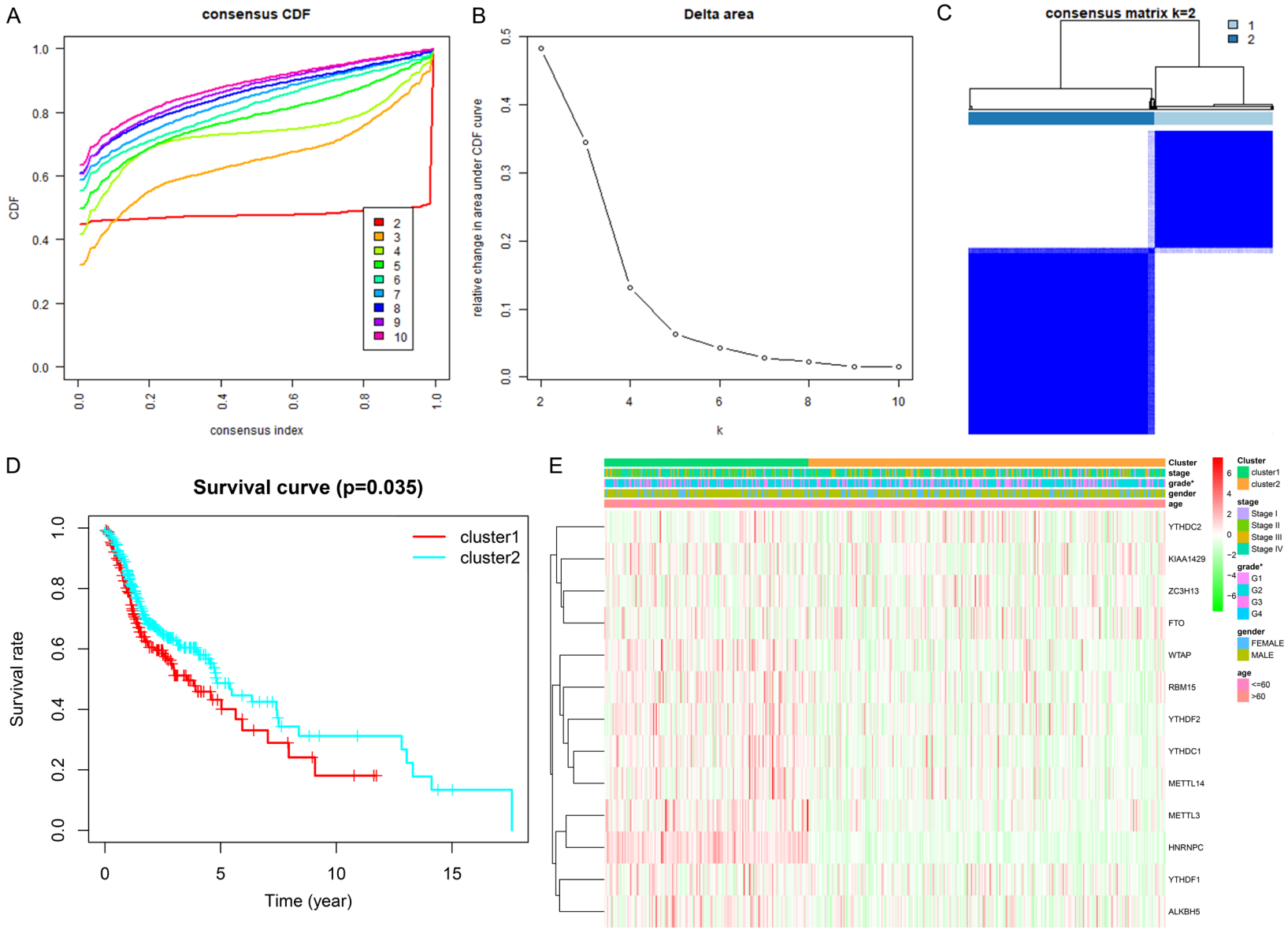

Figure 3. Differential overall survival and grade of TCGA HNSCC patients in the two different clusters. A. Consensus clustering cumulative distribution function (CDF) for k = 2 to 10. B. Relative change in area under CDF curve for k = 2 to 10. C. The TCGA HNSCC cohort was divided into two distinct clusters when k = 2. D. The OS in the cluster 1 was significantly shorter than that in the cluster 2. E. Significant difference was found for the grade between cluster 1 and cluster 2.

A

	pvalue	Hazard ratio
METTL3	0.138	0.951(0.889−1.016)
YTHDF1	0.952	1.001(0.979−1.023)
KIAA1429	0.916	1.003(0.944−1.066)
YTHDC2	0.007	0.847(0.751−0.955)
ALKBH5	0.629	1.003(0.990−1.017)
YTHDF2	0.722	1.005(0.980−1.030)
YTHDC1	0.168	0.969(0.926−1.014)
ZC3H13	0.610	1.015(0.958−1.077)
METTL14	0.824	1.019(0.864−1.201)
FTO	0.403	1.046(0.941−1.164)
WTAP	0.843	0.997(0.970−1.025)
RBM15	0.142	0.906(0.794−1.034)
HNRNPC	0.011	1.013(1.003−1.023)

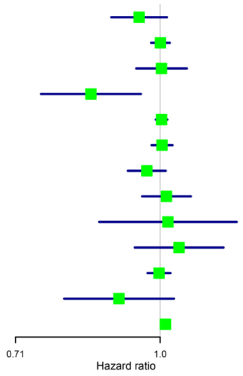

B

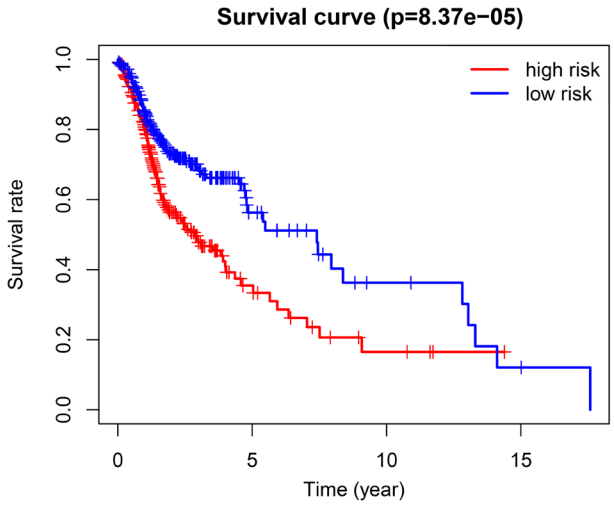

C

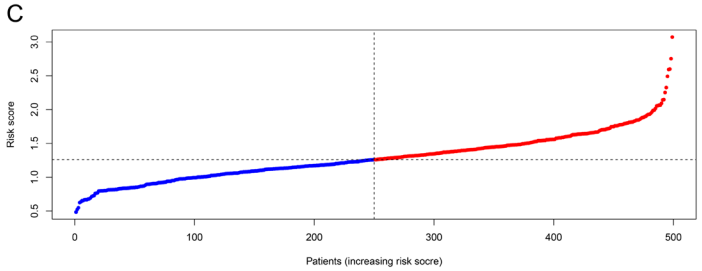

D

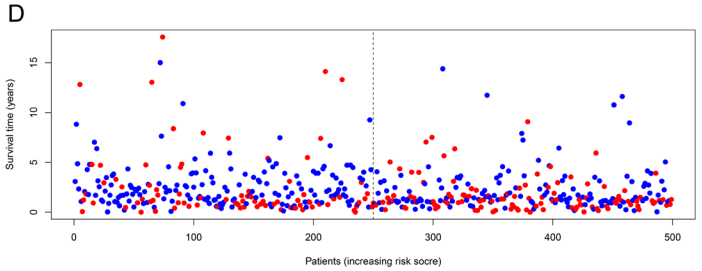

E

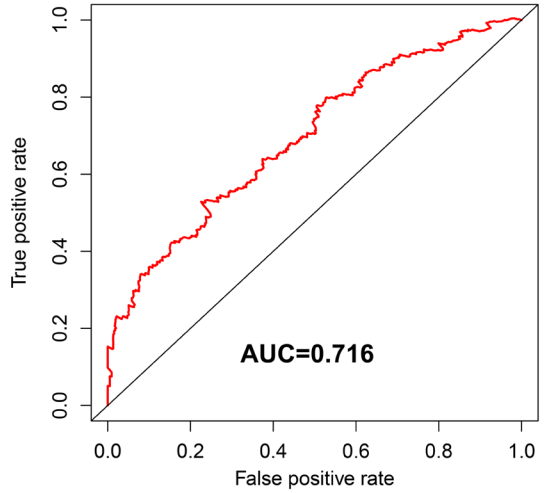

F

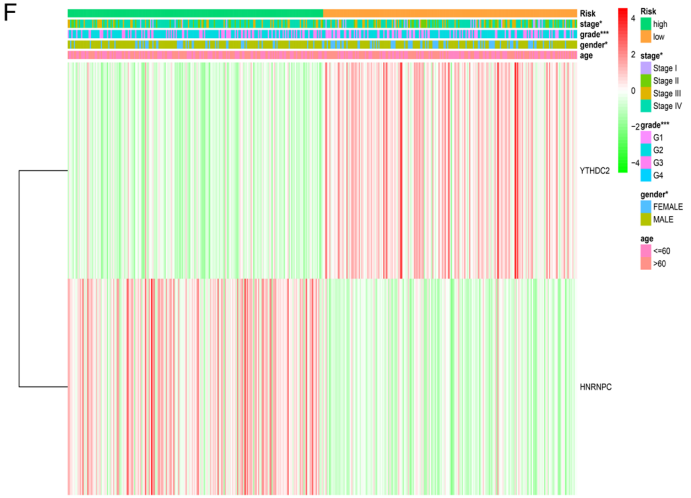

Figure 4. Construction of the prognostic signature based on TCGA HNSCC cohort. A. Univariate analysis of the m^{6}A RNA methylation regulators to identify the genes that significantly correlated with OS. B. The OS was remarkably shorter in the high-risk group than in low-risk group. C. The distributions of risk scores. D. The distributions of risk scores and OS status. The blue and red dots indicated the alive and dead status respectively. E. ROC curve was used to evaluate the prediction efficiency of the prognostic signature. F. Significant differences were found for the gender, grade and stage between high- and low-risk group.

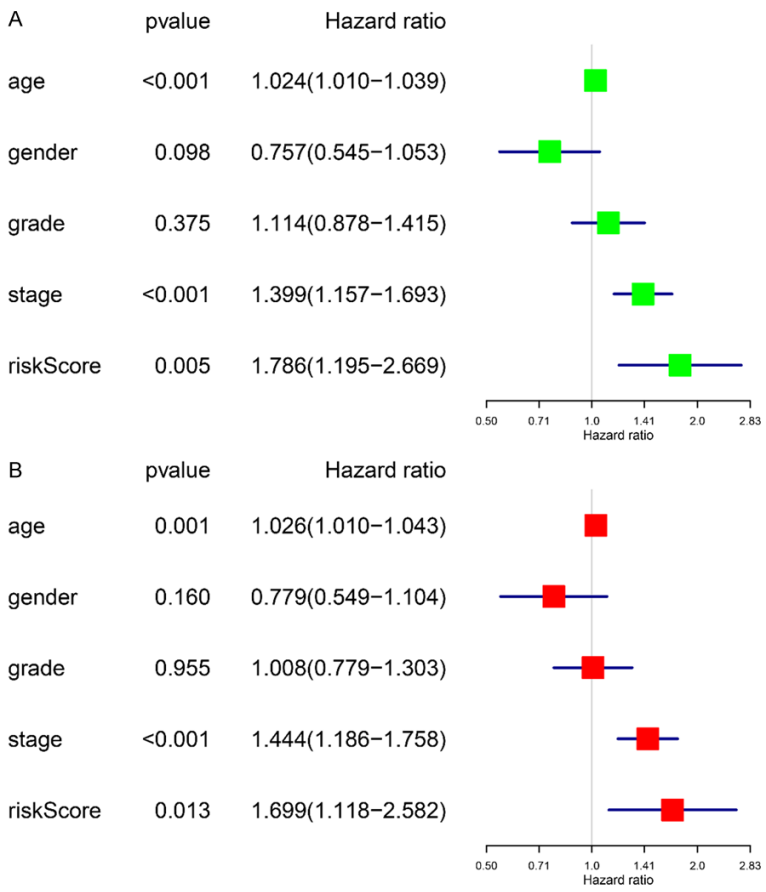

Figure 5. Identification of the independent prognostic factors in the TCGA HNSCC cohort. A. Univariate analysis of the risk score and clinicopathological parameters to identify the indicators that significantly correlated with OS. B. Multivariate analysis of the risk score and clinicopathological parameters to reveal the independent prognostic factors.

trols. Red or green color in the plots represented relatively high or low expression, respectively (**Figure 1A**). The expression levels of METTL3 (P < 0.001), YTHDF1 (P < 0.001), KIAA1429 (P < 0.001), ALKBH5 (P = 0.003), YTHDF2 (P = 0.045), METTL14 (P = 0.010), FTO (P = 0.005), WTAP (P < 0.001), RBM15 (P < 0.001) and HNRNPC (P < 0.001) were significantly overexpressed in tumor samples compared to normal control samples, while YTHDC2 (P = 0.025) was remarkably lower in the cancer specimens. No significant difference was found for YTHDC1 (P = 0.303) and ZC3H13 (P = 0.508) (**Figure 1B**).

The interaction and correlation among the m^{6}A RNA methylation regulators

The interactions among the thirteen m^{6}A RNA methylation regulators were shown in **Figure 2A**. WTAP and METTL14 seemed to be the hub genes of the interaction network. The results of the interaction network were further supported by the correlation analysis. Except for ALKBH5, WTAP was correlated with the other 11 m^{6}A RNA methylation regulators. METTL14 was associated with all the other 12 genes. Interestingly, METTL14 was most correlated with WTAP (r = 0.65) among all the interactions of m^{6}A RNA methylation regulators (**Figure 2B**).

Consensus clustering of m^{6}A RNA methylation regulators identified two clusters of HNSCC with different clinical outcomes

Based on the expression similarity of m^{6}A RNA methylation regulators, k = 2 was demonstrated to be the most appropriated selection to divide the HNSCC patient cohort into two clusters, namely cluster 1 and cluster 2 (**Figure 3A-C**). A significant shorter OS was observed in HNSCC patients in the cluster 1 than those in the cluster 2 (P = 0.035) (**Figure 3D**). Then the associations between the clustering and clinicopathological features were evaluated. Significant difference was found between the cluster 1 and cluster 2 for the grade (P < 0.05), while no significant difference was observed for other parameters such as age, gender and stage (**Figure 3E**).

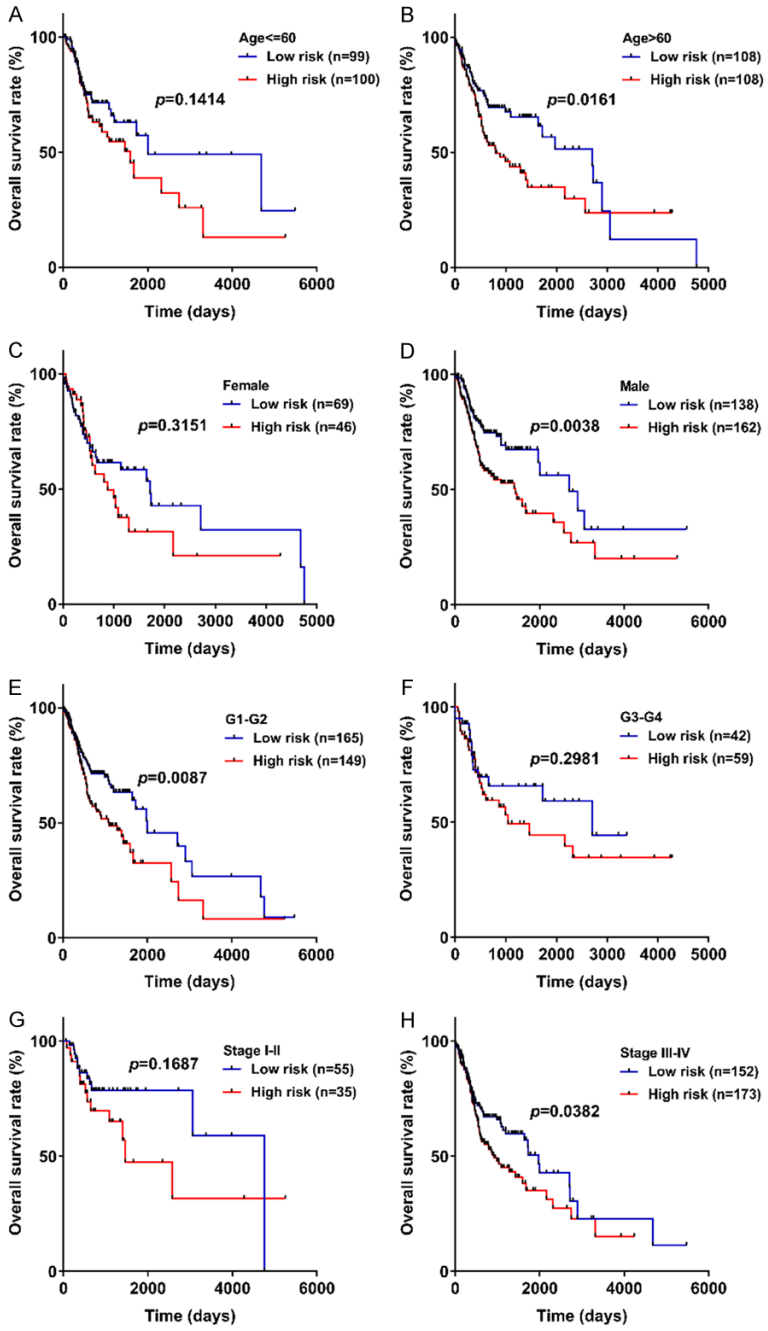

Figure 6. The survival difference between high- and low-risk group stratified by clinicopathological parameters in the TCGA HNSCC cohort. A, B. The difference in OS between high- and low-risk group stratified by age. C, D. The difference in OS between high- and low-risk group stratified by gender. E, F. The difference in OS between high- and low-risk group stratified by grade. G, H. The difference in OS between high- and low-risk group stratified by stage.

Identification of prognostic signature

Univariate Cox regression was used to identified the m^{6}A RNA methylation regulators that associated with OS in TCGA HNSCC cohort. The results demonstrated that YTHDC2 (P = 0.007) and HNRNPC (P = 0.011) were significantly correlated with OS. YTHDC2 was a protective gene with HR less than 1 (HR = 0.847, 95% CI = 0.751-0.955), and HNRNPC was a risky gene with HR larger than 1 (HR = 1.013. 95% CI = 1.003-1.023) (**Figure 4A**). These two genes were chosen to construct the prognostic signature and the coefficients were obtained from the LASSO algorithm. The risk score for each patient was calculated with the following formula: risk score = (-0.176) * YTHDC2 + (0.013) * HNRNPC. A total of 249 and 250 HNSCC patients were grouped into the high-risk group and low-risk group, respectively. The survival analysis showed that the HNSCC patients in the high-risk group had a significantly shorter overall survival than those in the low-risk group (P = 8.37e-05) (**Figure 4B**). **Figure 4C** showed the distributions of the two gene signature-based risk scores. The distributions of risk scores and OS status were displayed in **Figure 4D**. The prognostic signature model showed good prediction efficiency with the area under the ROC curve (AUC) value equal to 0.716 (**Figure 4E**). **Figure 4F** revealed that the expression of the YTHDC2 and HNRNPC in high- and low-risk group. Significant differences were found between the high- and low-risk groups with respect to gender (P < 0.05), grade (P < 0.001) and stage (P < 0.05).

The prognostic signature-based risk score was an independent prognostic factor in TCGA HNSCC cohort

Univariate and multivariate Cox regression analyses were performed to determine whether

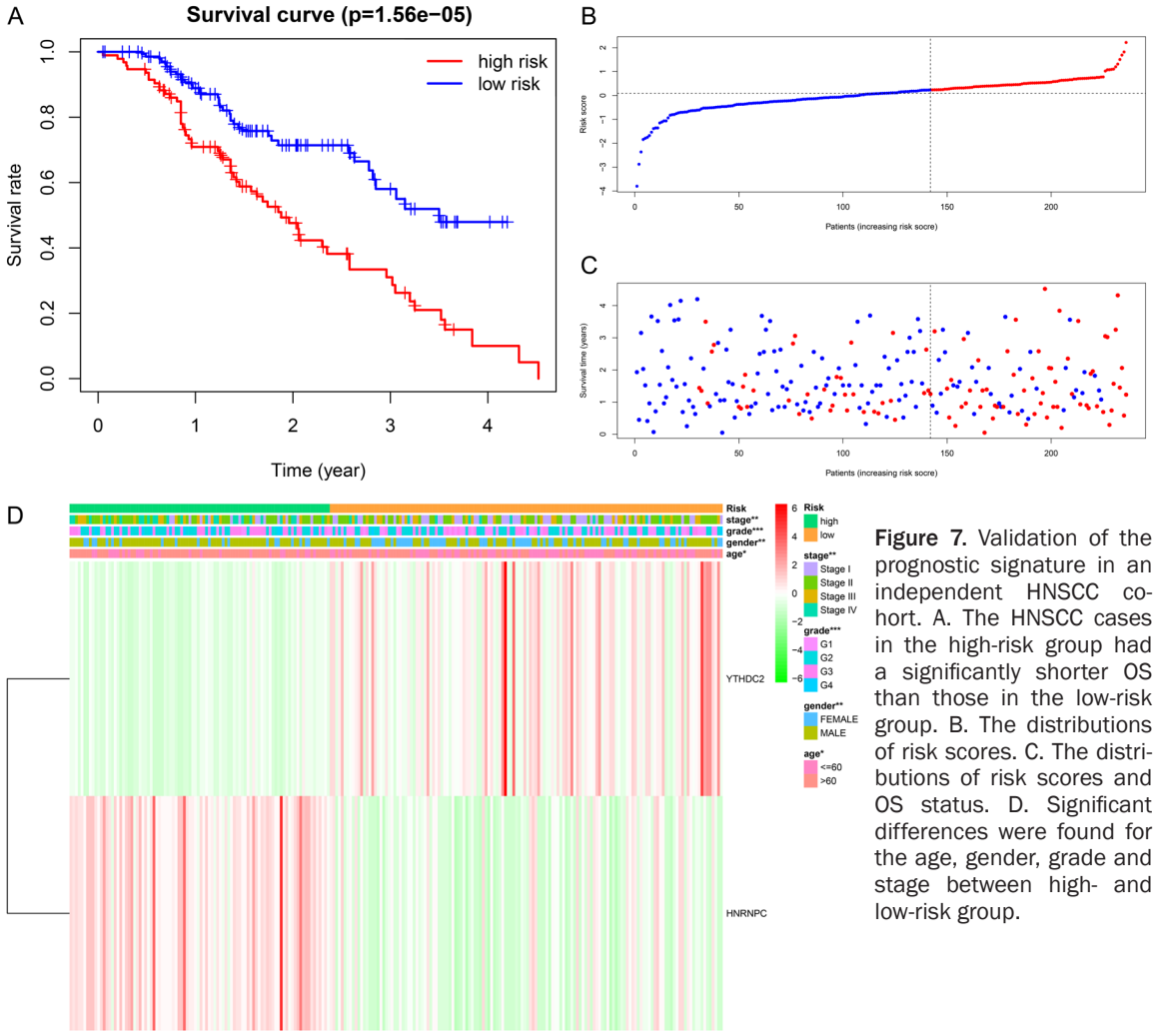

Figure 7. Validation of the prognostic signature in an independent HNSCC cohort. A. The HNSCC cases in the high-risk group had a significantly shorter OS than those in the low-risk group. B. The distributions of risk scores. C. The distributions of risk scores and OS status. D. Significant differences were found for the age, gender, grade and stage between high- and low-risk group.

the prognostic signature-based risk score was an independent prognostic indicator. After deleting cases with missing values in age, gender, grade or stage, a total of 415 cases were used for subsequent analysis. The univariate analysis showed that the age (P < 0.001, HR = 1.024, 95% CI = 1.010-1.039), stage (P < 0.001, HR = 1.399, 95% CI = 1.157-1.693) and risk score (P = 0.005, HR = 1.786, 95% CI = 1.195-2.669) were significantly correlated with the OS (**Figure 5A**). When these parameters were included into the multivariate Cox regression model, the age (P = 0.001, HR = 1.026, 95% CI = 1.010-1.043), stage (P < 0.001, HR = 1.444, 95% CI = 1.186-1.758) and risk score (P = 0.013, HR = 1.699, 95% CI = 1.118-2.582) were identified as the independent prognostic factors (**Figure 5B**).

The prognostic values of the risk signature for different clinicopathological parameters including age, gender, grade and stage were further investigated. As shown in **Figure 6A-H**, high-risk group had significantly shorter OS than those in the low-risk group for the cases with age > 60 (P = 0.0161), or male cases (P = 0.0038), or patients at the G1-G2 (P = 0.0087) or those at the stage III-IV (P = 0.0382). However, no significant difference was found for OS between high- and low-risk groups for the HNSCC patients with age ≤ 60 (P = 0.1414), or female cases (P = 0.3151), or patients at the G3-G4 (P = 0.2981), or those at the stage I-II (P = 0.1687).

Validation of the prognostic signature

A total of 236 cases were included in the validated HNSCC cohort. Based on the cut-off value of the risk scores, 94 patients were categorized into high-risk group and the remaining 142 cases were grouped into low-risk group.

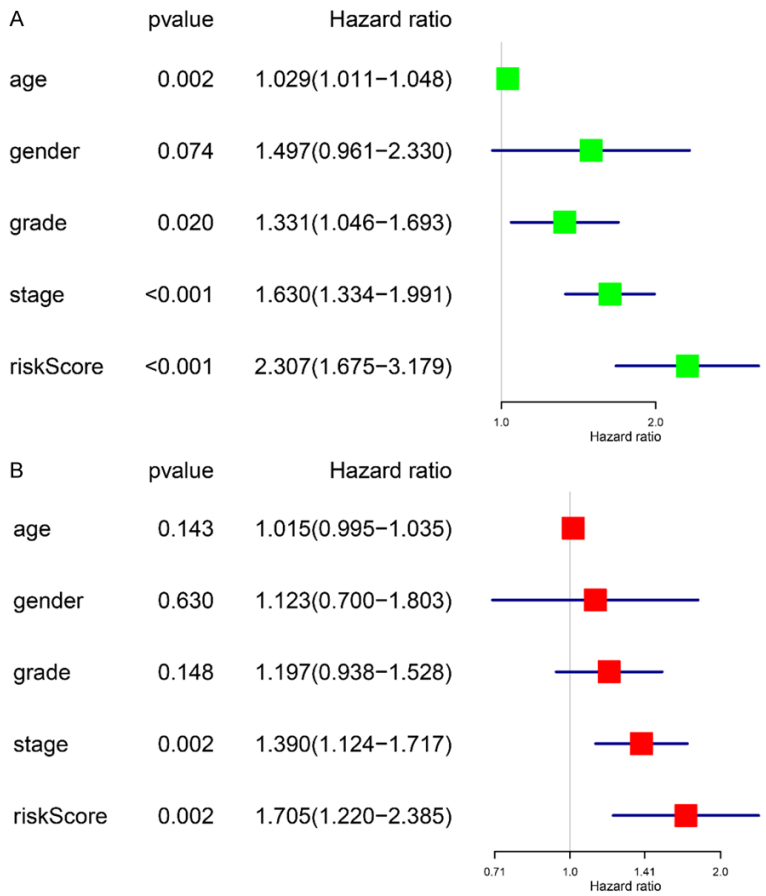

Figure 8. Identification of the independent prognostic factors in the validated HNSCC cohort. A. Univariate analysis of the risk score and clinicopathological parameters to identify the indicators that significantly associated with OS. B. Multivariate analysis of the risk score and clinicopathological parameters to reveal the independent prognostic factors.

The survival analysis showed that the OS was significantly shorter in the high-risk group compared to that in the low-risk group (P = 1.56e-05) (**Figure 7A**). The distributions of the risk scores, OS and OS status were shown in **Figure 7B** and **7C**. Significant differences were observed for various clinicopathological parameters such as age (P < 0.05), gender (P < 0.01), grade (P < 0.001) and stage (P < 0.01) between high and low-risk group (**Figure 7D**). Univariate analysis revealed that the age (P = 0.002, HR = 1.029, 95% CI = 1.011-1.048), grade (P = 0.020, HR = 1.331, 95% CI = 1.046-1.693), stage (P < 0.001, HR = 1.630, 95% CI = 1.334-1.991) and risk score (P < 0.001, HR = 2.307, 95% CI = 1.675-3.179) were significantly associated with the OS (**Figure 8A**). Multivariate analysis showed that stage (P = 0.002, HR = 1.390, 95% CI = 1.124-1.717) and risk score (P = 0.002, HR = 1.705, 95% CI = 1.220-2.385) were independent prognostic indicators (**Figure 8B**). As shown in **Figure 9A-H**, the OS rate was significantly lower in the high-risk group compared to that in the low-risk group for the cases with age > 60 (P = 0.0007), or cases with age ≤ 60 (P = 0.0040), or male cases (P < 0.0001), or patients at the G1-G2 (P = 0.0338), or patients at the G3-G4 (P = 0.0109) or those at the stage I-II (P < 0.0001). However, no significant difference was found for OS between high- and low-risk groups for the female cases (P = 0.2637), or patients at the stage III-IV (P = 0.2726).

Discussion

The initiation and development of HNSCC is a multistep process that involves gradually acquisition of genetic and epigenetic alterations, leading to uncontrolled growth and proliferation of tumor cells. Therefore, elucidating the underlying molecular events accounting for the tumorigenesis of HNSCC is important. Aberrant m^{6}A RNA methylation modifications have been demonstrated to regulate carcinogenesis of many tumor types. However, their role in HNSCC is unclear. In this study, we found that most m^{6}A RNA methylation regulators were abnormally expressed in HNSCC. In addition, based on the expression pattern of the thirteen m^{6}A RNA methylation regulators, the TCGA HNSCC cohort could be divided into two subgroups with significant differences for OS and tumor grade. Moreover, based on TCGA HNSCC dataset, a robust risk signature including YTHDC2 and HNRNPC was constructed and showed good performance for predicting the clinical outcome of HNSCC. More importantly, this two-gene signature was further successfully validated as an independent prognostic marker in an external independent HNSCC cohort, indicating that this prognostic model is highly robust for prognosis prediction.

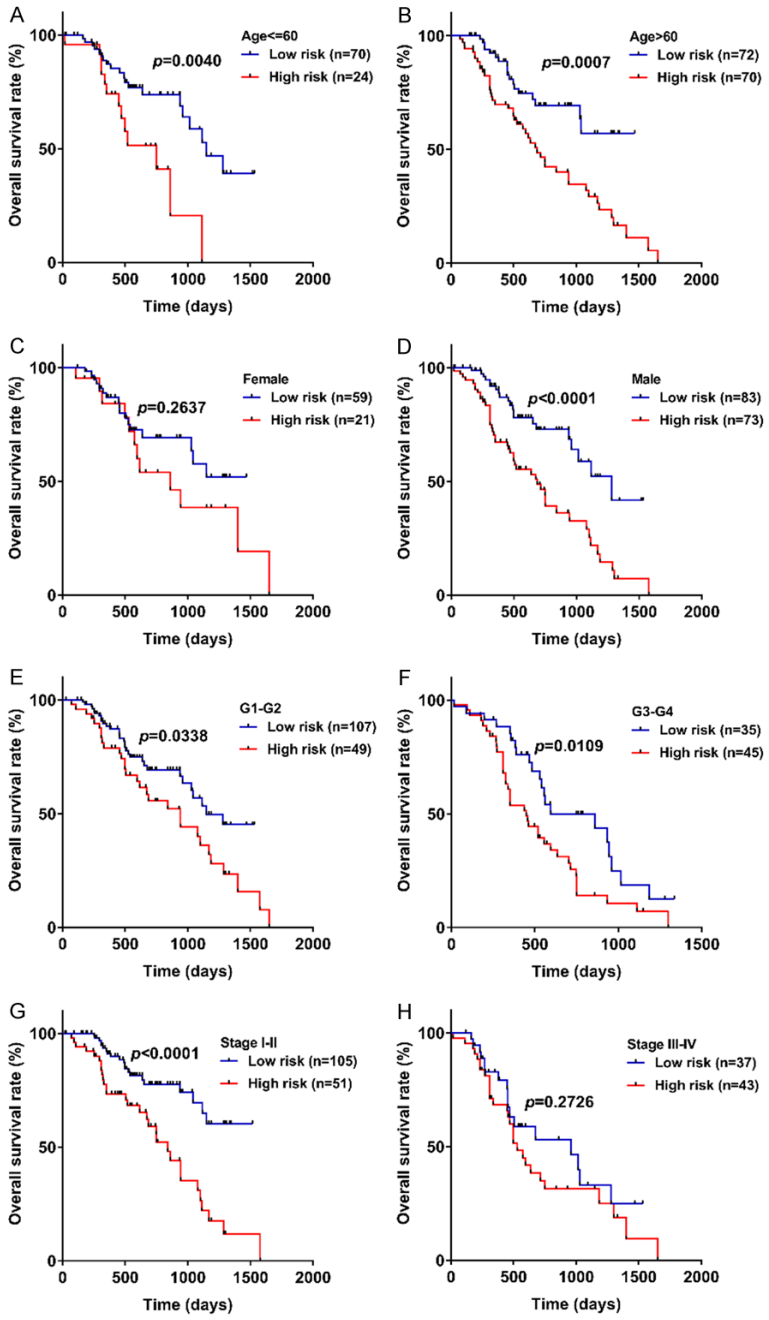

Figure 9. The survival difference between high- and low-risk group stratified by clinicopathological parameters in the validated HNSCC cohort. A, B. The difference in OS between high- and low-risk group stratified by age. C, D. The difference in OS between high- and low-risk group stratified by gender. E, F. The difference in OS between high- and low-risk group stratified by grade. G, H. The difference in OS between high- and low-risk group stratified by stage.

Consistent with the findings from previous studies, m^{6}A RNA methylation regulators are aberrantly expressed in many types of cancers. For instance, the expression levels of WTAP were elevated in AML samples and cell lines. In addition, knock down of WTAP suppressed the proliferation and survival of AML cells, indicating that WTAP might act as an oncogene in AML [17]. Similarly, METTL3 was upregulated in the bladder cancer tissue samples. Downregulation of METTL3 inhibited the proliferation, migration, invasion capacity of cancer cells in vitro and tumor growth in vivo, and vice versa [18]. Our findings showed that 11 out of 13 m^{6}A RNA methylation regulators were upregulated or downregulated in the HNSCC samples, suggesting that these genes might be associated with the oncogenic activities of cancer cells and/or prognosis of HNSCC patients. Further studies are warranted to determine the underlying molecular mechanisms.

Interestingly, two HNSCC subgroups were identified by consensus clustering based on the expression of m^{6}A RNA methylation regulators. The OS and tumor grade were dramatically different between the two subgroups, indicating that the levels of m^{6}A RNA methylation regulators are closely associated with unfavorable prognosis of HNSCC. One of the major findings in the current study was that the two-gene risk signature including YTHDC2 and HNRNPC was built up and demonstrated to robustly predicts the prognosis of patients with HNSCC from different independent cohorts. Although no significant difference was found for OS between high- and low-risk group when the two HNSCC cohorts were stratified by some clinicopathological features, the trend that the high-risk group suffered a more unfavorable clinical outcome compared to the low-risk group could

still be observed. We speculated that increasing the sample size might contribute to detect the potential statistical significance.

Our prognostic model showed that the expression level of YTHDC2 was positively associated with the prognosis of HNSCC, indicating that YTHDC2 might act as a tumor suppressor gene in HNSCC. Currently, little information is available for the role of YTHDC2 in tumorigenesis. Tanabe et al reported that YTHDC2 was positively associated with the progression of colon cancer and promoted the malignant ability of colon cancer cells, suggesting that YTHDC2 might play an oncogenic role in carcinogenesis of CRC [19]. Similarly, downregulation of YTHDC2 suppressed the growth capability of hepatocellular carcinoma cell line [20]. It is entirely possible that m^6A RNA methylation regulators play contradictory roles in different types of cancers or even in the same tumor type. For instance, METTL3 acted as a tumor suppressor gene in endometrial cancer and glioblastoma, while functioned as an oncogene in bladder cancer [14, 18, 21]. On the contrary, the expression of the other gene HNRNPC was negatively correlated with OS in HNSCC, suggesting that HNRNPC might be a promoter for HNSCC tumorigenesis. Alternative cleavage and polyadenylation (APA) is a common phenomenon which enhances the cellular repertoire of mRNA isoforms. HNRNPC overexpression was found in CRC cells and the major regulator of cancer progression related genes by modifying APA profiles [22]. The expression level of HNRNPC was higher in highly invasive GBM cell line and HNRNPC upregulation was associated with tumor grade. In addition, knock down of HNRNPC reduced cell proliferation and enhanced etoposide-induced apoptosis, indicating HNRNPC acted as an oncogene in GBM [23]. Similarly, HNRNPC overexpression was closely with the chemoresistance of gastric cancer cells. High level of HNRNPC was correlated with unfavorable clinical outcome [24].

Conclusion

Collectively, our study has profiled the dramatically altered m^6A RNA methylation regulators between HNSCC and normal controls, which might play a crucial role in the progression of HNSCC. More importantly, a robust prognostic signature that significantly associated with the unfavorable clinical outcome of HNSCC was constructed and validated in two different independent HNSCC cohorts, indicating that this prognostic signature might serve as promising molecular biomarkers for monitoring HNSCC development and provide important guidance for selecting therapeutic strategies.

Acknowledgements

This study was supported by the grants from National Natural Science Foundation of China (No. 81901006) and Medical Scientific Research Foundation of Guangdong Province of China (No. A2019299).

Disclosure of conflict of interest

None.

Address correspondence to: Dr. Xinyuan Zhao, Stomatological Hospital, Southern Medical University, Guangzhou 510280, China. Tel: +86-2084418217; E-mail: zhaoxinyuan1989@smu.edu.cn; Dr. Li Cui, UCLA School of Dentistry, Los Angeles, CA 90095, USA. Tel: +310-206-8834; E-mail: zsucllj@ucla.edu

References

[1] Liu XZ, Zhao XY and Gou CY. Identification of novel methylated DNA marker ZNF569 for head and neck squamous cell carcinoma. J Cancer 2019; 10: 2250-2260.

[2] Forastiere A, Koch W, Trotti A, Sidransky D. Head and neck cancer. N Engl J Med 2001; 345: 1890-1900.

[3] Sanderson RJ and Ironside JA. Squamous cell carcinomas of the head and neck. BMJ 2002; 325: 822-827.

[4] Huang J, Ji EH, Zhao X, Cui L, Misuno K, Guo M, Huang Z, Chen X and Hu S. Sox11 promotes head and neck cancer progression via the regulation of SDCCAG8. J Exp Clin Cancer Res 2019; 38: 138.

[5] Yue Y, Liu J, He C. RNA N6-methyladenosine methylation in post-transcriptional gene expression regulation. Genes Dev 2015; 29: 1343-1355.

[6] Chen XY, Zhang J, Zhu JS. The role of m^6A RNA methylation in human cancer. Mol Cancer 2019; 18: 103.

[7] Sun T, Wu R, Ming L. The role of m6A RNA methylation in cancer. Biomed Pharmacother 2019; 112: 108613.

[8] Yang Y, Hsu PJ, Chen YS, Yang YG. Dynamic transcriptomic m^6A decoration: writers, erasers, readers and functions in RNA metabolism. Cell Res 2018; 28: 616-624.

[9] Geula S, Moshitch-Moshkovitz S, Dominissini D, Mansour AA, Kol N, Salmon-Divon M, Hershkovitz V, Peer E, Mor N, Manor YS, Ben-Haim MS, Eyal E, Yunger S, Pinto Y, Jaitin DA, Viukov S, Rais Y, Krupalnik V, Chomsky E, Zerbib M, Maza I, Rechavi Y, Massarwa R, Hanna S, Amit I, Levanon EY, Amariglio N, Stern-Ginossar N, Novershtern N, Rechavi G, Hanna JH. Stem cells. m6A mRNA methylation facilitates resolution of naive pluripotency toward differentiation. Science 2015; 347: 1002-1006.

[10] Fustin JM, Doi M, Yamaguchi Y, Hida H, Nishimura S, Yoshida M, Isagawa T, Morioka MS, Kakeya H, Manabe I, Okamura H. RNA-methylation-dependent RNA processing controls the speed of the circadian clock. Cell 2013; 155: 793-806.

[11] Mendel M, Chen KM, Homolka D, Gos P, Pandey RR, McCarthy AA, Pillai RS. Methylation of structured RNA by the m^{6}A writer METTL16 is essential for mouse embryonic development. Mol Cell 2018; 71: 986-1000.

[12] Xiang Y, Laurent B, Hsu CH, Nachtergaele S, Lu Z, Sheng W, Xu C, Chen H, Ouyang J, Wang S, Ling D, Hsu PH, Zou L, Jambhekar A, He C, Shi Y. RNA m^{6}A methylation regulates the ultraviolet-induced DNA damage response. Nature 2017; 543: 573-576.

[13] Wei WQ, Ji XY, Guo XQ, Ji SP. Regulatory role of N^6-methyladenosine (m^{6}A) methylation in RNA processing and human diseases. J Cell Biochem 2017; 118: 2534-2543.

[14] Cui Q, Shi H, Ye P, Li L, Qu Q, Sun G, Sun G, Lu Z, Huang Y, Yang CG, Riggs AD, He C, Shi Y. m^{6}A RNA Methylation regulates the self-renewal and tumorigenesis of glioblastoma stem cells. Cell Rep 2017; 18: 2622-2634.

[15] Chen J, Sun Y, Xu X, Wang D, He J, Zhou H, Lu Y, Zeng J, Du F, Gong A, Xu M. YTH domain family 2 orchestrates epithelial-mesenchymal transition/proliferation dichotomy in pancreatic cancer cells. Cell Cycle 2017; 16: 2259-2271.

[16] Zhao XY, Sun SY, Zeng XQ, Cui L. Expression profiles analysis identifies a novel three-mRNA signature to predict overall survival in oral squamous cell carcinoma. Am J Cancer Res 2018; 8: 450-461.

[17] Bansal H, Yihua Q, Iyer SP, Ganapathy S, Proia D, Penalva LO, Uren PJ, Suresh U, Carew JS, Karnad AB, Weitman S, Tomlinson GE, Rao MK, Kornblau SM, Bansal S. WTAP is a novel oncogenic protein in acute myeloid leukemia. Leukemia 2014; 28: 1171-1174.

[18] Cheng M, Sheng L, Gao Q, Xiong Q, Zhang H, Wu M, Liang Y, Zhu F, Zhang Y, Zhang X, Yuan Q, Li Y. The m^{6}A methyltransferase METTL3 promotes bladder cancer progression via AFF4/NF-kappaB/MYC signaling network. Oncogene 2019; 38: 3667-3680.

[19] Tanabe A, Tanikawa K, Tsunetomi M, Takai K, Ikeda H, Konno J, Torigoe T, Maeda H, Kutomi G, Okita K, Mori M, Sahara H. RNA helicase YTHDC2 promotes cancer metastasis via the enhancement of the efficiency by which HIF-1 alpha mRNA is translated. Cancer Lett 2016; 376: 34-42.

[20] Tanabe A, Konno J, Tanikawa K, Sahara H. Transcriptional machinery of TNF-alpha-inducible YTH domain containing 2 (YTHDC2) gene. Gene 2014; 535: 24-32.

[21] Liu J, Eckert MA, Harada BT, Liu SM, Lu Z, Yu K, Tienda SM, Chryplewicz A, Zhu AC, Yang Y, Huang JT, Chen SM, Xu ZG, Leng XH, Yu XC, Cao J, Zhang Z, Liu J, Lengyel E, He C. m^{6}A mRNA methylation regulates AKT activity to promote the proliferation and tumorigenicity of endometrial cancer. Nat Cell Biol 2018; 20: 1074-1083.

[22] Fischl H, Neve J, Wang Z, Patel R, Louey A, Tian B, Furger A. hnRNPC regulates cancer-specific alternative cleavage and polyadenylation profiles. Nucleic Acids Res 2019; 47: 7580-7591.

[23] Park YM, Hwang SJ, Masuda K, Choi KM, Jeong MR, Nam DH, Gorospe M, Kim HH. Heterogeneous nuclear ribonucleoprotein C1/C2 controls the metastatic potential of glioblastoma by regulating PDCD4. Mol Cell Biol 2012; 32: 4237-4244.

[24] Huang H, Han Y, Zhang C, Wu J, Feng JN, Qu LK, Shou CC. HNRNPC as a candidate biomarker for chemoresistance in gastric cancer. Tumor Biol 2016; 37: 3527-3534.